Colloids and Surfaces A: Physicochem. Eng. Aspects 461 (2014) 92–97

Contents lists available at ScienceDirect

Colloids and Surfaces A: Physicochemical and Engineering Aspects

journal homepage: www.elsevier.com/locate/colsurfa

Preparation of hybrid thin films by a green synthesis method and their application

Bihua Xia, Xiaoyu Wang, Lidong Li*

School of Materials Science and Engineering, University of Science and Technology Beijing, Beijing 100083, PR China

HIGHLIGHTS

- Hybrid thin film was prepared by *in situ* reduction and self-assembly technique.
- The hybrid film showed good antibacterial activity.
- The hybrid film exhibited metal-enhanced fluorescence effect.

GRAPHICAL ABSTRACT

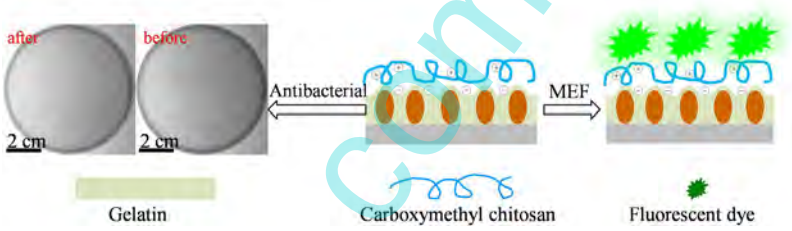

ARTICLE INFO

Article history:
Received 2 May 2014
Received in revised form 8 July 2014
Accepted 21 July 2014
Available online 29 July 2014

Keywords:
Self-assembly
Fluorescence
Nanoparticles
Hybrid materials
Green synthesis
Antibacterial

ABSTRACT

Hybrid thin biomacromolecular films were fabricated by combining the *in situ* formation of silver nanoparticles (Ag NPs) in gelatin and self-assembly of carboxymethyl chitosan (CCHI). The hybrid films exhibited excellent antibacterial activity toward *Escherichia Coli*. When the fluorescent dye 4,7-(9,9′-bis(6-adenine hexyl)fluorenyl)-2,1,3-benzothiadiazole modified with nucleotide adenine and quaternary ammonium groups (OFBT-AA) was adsorbed onto the surface of the hybrid films, metal-enhanced fluorescence resulted in a maximum 5.3-fold increase in the fluorescence of OFBT-AA.

1. Introduction

Biomacromolecular films are important for a variety of applications in pharmaceutical coatings, drug delivery and biomedical science [1–3]. Several functional biomacromolecular films have been prepared from polysaccharides, proteins and synthetic polymers [4,5]. Among these natural materials, gelatin is an ideal material to prepare biomaterial films because of its biocompatibility, biodegradability, abundance, and curing characteristic [6]. Moreover, gelatin molecules contain many kinds of amino acids, which have reduction activity and can reduce silver (Ag^+) ions [7].

To date, silver nanoparticles (Ag NPs) with different morphologies and sizes have been prepared by techniques such as mechanical lapping [8], thermal decomposition [9], laser ablation [10], microwave irradiation and sonochemical synthesis [11]. However, the method used most commonly to fabricate Ag NPs is the chemical reduction of metal salts [12,13]. This method normally involves reduction of an ionic salt in an organic medium using a chemical reducing agent [14–16]. To avoid introduction of toxic chemicals, environmentally friendly, nontoxic and biocompatible green materials have been used to prepare Ag NPs in recent years [17–19]. However, using gelatin as the reduction agent for fabricate Ag NPs was scarcely reported [20].

* Corresponding author. Tel.: +86 10 82377202; fax: +86 10 82375712.
E-mail address: lidong@mater.ustb.edu.cn (L. Li).

http://dx.doi.org/10.1016/j.colsurfa.2014.07.025
0927-7757/

Ag NPs with large relative surface area and strong surface activity exhibit good antibacterial properties. They can damage the cell membrane of microorganisms to induce decomposition and complete destruction [21,22]. Several kinds of Ag NPs composite film preparation methods have been reported, for example, solvent casting method [23], sol–gel method followed by photo-reduction [24]. Some prepared film systems also showed good antibacterial performance [25], but the antibacterial performance of Ag NP hybrid films prepared using gelatin by a simply *in situ* reduction method has not been examined.

Because of their obvious surface plasmon resonance effect, Ag NP films have been fabricated in film systems for metal-enhanced fluorescence (MEF) applications, with large enhancement effects being achieved [26–28]. MEF can be controlled by designing a metallic nanostructure with an appropriate interaction region. Our group has also reported several distance-controlled MEF systems [29–31]. However, few reports have used biomolecular systems to realize MEF.

In this work, a green synthesis method to prepare Ag NPs is developed that simultaneously uses gelatin as the reduction agent and stabilizer. Gelatin-Ag NP films are produced by self-assembly and cooling solidification, and then carboxymethyl chitosan (CCHI) molecules are absorbed on the surface of the gelatin-Ag NPs film through electrostatic interaction to give Ag NP hybrid films. The antibacterial properties of these hybrid films are evaluated using *Escherichia Coli* (*E. Coli*). The π-conjugated oligomer 4,7-(9,9′-bis(6-adenine hexyl)fluorenyl)-2,1,3-benzothiadiazole modified with nucleotide adenine and quaternary ammonium groups (OFBT-AA) is used as a model dye to examine the MEF performance of the hybrid films.

2. Experimental

2.1. Materials

Gelatin, silver nitrate ($AgNO_3$), carboxymethyl chitosan (CCHI) and pancreatin (USP grade) were purchased from Aladdin Chemistry Co., Ltd. OFBT-AA was synthesized according to a published method [32,33]. The molecular structures of CCHI and OFBT-AA were showed in Scheme 1. Yeast extract, tryptone, and dextrose (YTD) agar were purchased from Sigma–Aldrich. *E. Coli* and the antibiotic ampicillin were purchased from Tiangen Biotechnology Co., Ltd. Deionized water was purified using a Millipore filtration system. All reagents were used without further purification unless otherwise stated.

2.2. Measurements

UV–vis absorption spectra were measured on spectrophotometers (JASCO V-550 and Hitachi U3900). The film thicknesses were measured by interference microscope (6J-690162). Transmission electron microscope (TEM) images were recorded on a TEM (JEM 2100) with an accelerating voltage of 200 kV. Field-emission scanning electron microscopy (FE-SEM) images were recorded on a FE-SEM (Quanta 200FEG) with an accelerating voltage of 4.0–6.0 kV. Atomic force microscope (AFM) image was obtained from a CSPM5000 microscope operating in tapping mode.

2.3. Preparation of gelatin-reduced Ag NP colloids

Deionized water (60 mL) and gelatin powder (8 g) were mixed and then heated to 80 °C to dissolve the gelatin. $AgNO_3$ (0.1, 0.3, 0.5 or 0.7 g) was added rapidly to the aqueous gelatin solution with vigorous stirring. The reaction flask was coated with tinfoil to minimize light exposure. The mixture was heated at 95 °C for 1 h in an oil bath to give a brown gelatin-Ag NP solution. The gelatin-coated Ag NPs are referred to as gelatin-Ag NPs-0.1, gelatin-Ag NPs-0.3, gelatin-Ag NPs-0.5 and gelatin-Ag NPs-0.7 for samples prepared using 0.1, 0.3, 0.5 and 0.7 g of $AgNO_3$, respectively.

2.4. Preparation of Ag NP-containing hybrid films

Quartz (SiO_2) slides (30 mm × 10 mm) were immersed in piranha solution (H_2O_2:H_2SO_4 = 1:3 *v*/*v*) for 2 h, washed three times with deionized water, and then dried under a gentle stream of nitrogen gas. Ag NP-containing hybrid films were fabricated on the quartz substrates by self-assembly. The cleaned quartz slides were placed in the gelatin-Ag NP colloid solutions at 60 °C for 1 h, taken out and cooled for 10 min at room temperature. The films were immersed in 1.5% (*w*/*w*) aqueous solution of CCHI for 10 min to absorb CCHI molecules through electrostatic attraction and cross-linking reactions [34]. The Ag NP hybrid film-coated quartz slides were heated at 45 °C for 1 h to evaporate water.

2.5. Antibacterial experiments

Antibacterial experiments were performed following a reported method [35]. The antibacterial performance of the Ag NP hybrid films and gelatin-CCHI films was determined by incubation with *E. Coli* (Gram-negative bacteria) suspensions at 30 °C for 30 min in the dark, and then the *E. Coli* suspensions were serially diluted 1×10^4-fold with PBS. Aliquots (100 μL) of the diluted *E. Coli* suspension were spread on a solid YTD agar plate, and the colonies formed after incubation at 37 °C for 24 h were counted. The survival fraction was determined by dividing the number of colony-forming units (cfu) of the samples incubated with Ag NP hybrid film (10 mm × 10 mm) or gelatin-CCHI film (10 mm × 10 mm) by the number of cfu of the control prepared in the absence of any film. The diameter of the solid agar plates was 90 mm. The inhibition ratio (IR) of *E. Coli* was calculated according to the following equation: $IR = [(C_0 - C)/C_0] \times 100\%$

where C is the cfu of the experimental group treated with Ag NP hybrid film or gelatin-CCHI film, and C_0 is the cfu of the control group without any film.

2.6. Fluorescence spectra

To investigate the MEF of the Ag NP hybrid films, OFBT-AA aqueous solution (2 μL, 1 mM) was added dropwise onto the dry Ag NP hybrid and gelatin-CCHI films. The films were dried under a flow of air at room temperature for 2 h. Fluorescence spectra were measured on a fluorometer (Hitachi F-7000) using a xenon lamp as the excitation source.

3. Results and discussion

3.1. Synthesis and characterization of gelatin-Ag NP films

Gelatin is a heterogeneous mixture of high-molecular-weight water-soluble proteins derived from partial hydrolysis of naturally occurring collagen, and contains relatively high amounts of non-polar amino acids [36]. These amino acid molecules contain functional groups such as $-NH_2$ and –SH, so they can reduce Ag^+ ions to form silver colloids [20]. In this work, we used gelatin as the reduction agent and stabilizer to prepare Ag NPs. $AgNO_3$ was added to an aqueous solution of gelatin, which was heated at 95 °C for 1 h to give gelatin-reduced Ag NP colloids. Because of their surface plasmon resonance effect, we measured the UV–vis spectra of the gelatin-reduced Ag NP colloids (Fig. 1a). The intensity of surface plasmon absorption increased as more $AgNO_3$ was added to the gelatin solution, and more Ag ions were reduced to Ag colloids as the concentration of Ag^+ increased. The absorption peaks of the Ag NP colloids were all located at around 440 nm. This result is mainly

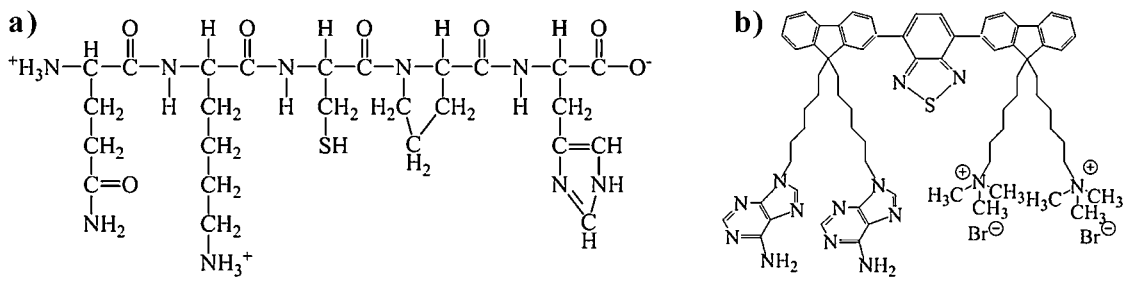

Scheme 1. Molecular structures of (a) gelatin and (b) OFBT-AA.

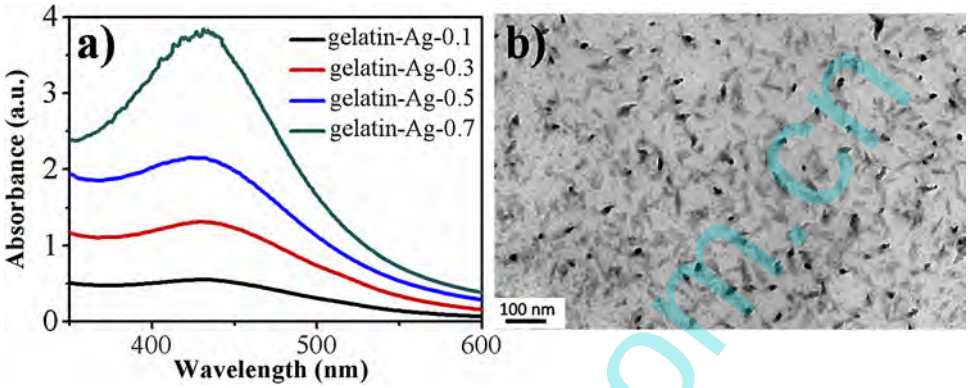

Fig. 1. (a) UV–vis absorption spectra of gelatin-reduced Ag NP colloids, and (b) TEM image of a gelatin-Ag NPs-0.7 film.

attributed to the limiting effect of gelatin, which has a triple-helix structure in aqueous solution [37], so it can control the growth of Ag NPs [38].

Exploiting the ability of gelatin to solidify, we made gelatin-Ag NP films by self-assembly. Cleaned quartz slides were immersed in gelatin-Ag NP colloid solution at 60 °C for 1 h, took out and cooled to room temperature, then heated up to 45 °C for 1 h to obtain a gelatin-Ag NP film. By interference microscope, the thickness of gelatin-Ag NP film was obtained about 1.2 μm. A TEM image of a gelatin-Ag NPs-0.7 film is presented in Fig. 1b. The film is continuous on the quartz slide; Ag NPs are embedded in the solid gelatin and densely packed. The Ag NPs were rod-like with a cross section and length of about 10 and 60 nm, respectively. The blank gray and dark regions in this film show the Ag NPs inside and outside gelatin, respectively. To better characterize their surface structure, we also captured FE-SEM images of gelatin and gelatin-Ag NPs-0.7 films (Fig. 2). The gelatin film had a very flat surface, whereas that of the gelatin-Ag NPs film was rough. This difference resulted from the *in situ*-generated Ag NPs in the gelatin-Ag NPs-0.7 film. In addition, the surface topographies of gelatin-Ag NPs-0.7 film after AFM measurement is shown in Fig. 3. The gelatin-Ag NPs film exhibited an inhomogeneous phase with roughness surface, and this phenomenon was mainly due to the Ag NPs embedding in gelatin film. Because of the amphiprotic nature of gelatin, so this film should have the ability to interact with positively charged molecules such as chitosan through electrostatic attraction [22]. The strong surface plasmon resonance of these gelatin-Ag NP films means they are suitable for MEF applications [39,40].

3.2. Antibacterial studies

CCHI is a derivative of chitosan, which is a polysaccharide biopolymer that is nontoxic, biodegradable, biocompatible and bioactive, with multiple functional groups and antimicrobial

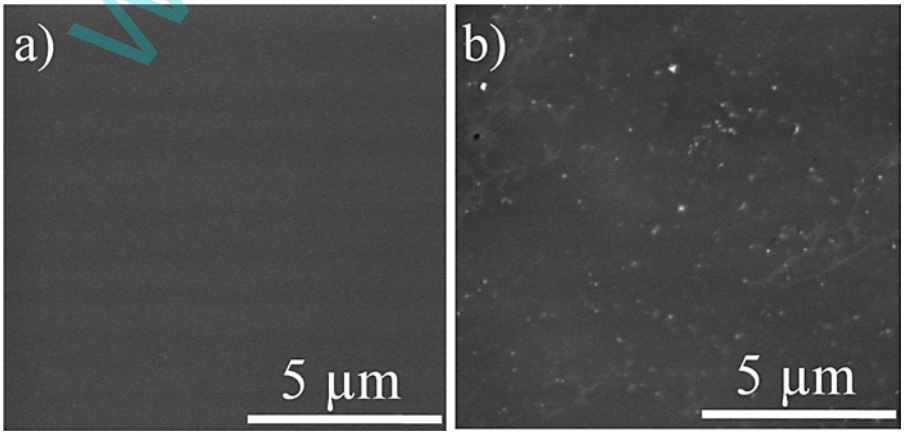

Fig. 2. FE-SEM images of (a) gelatin film and (b) gelatin-Ag NPs-0.7 film.

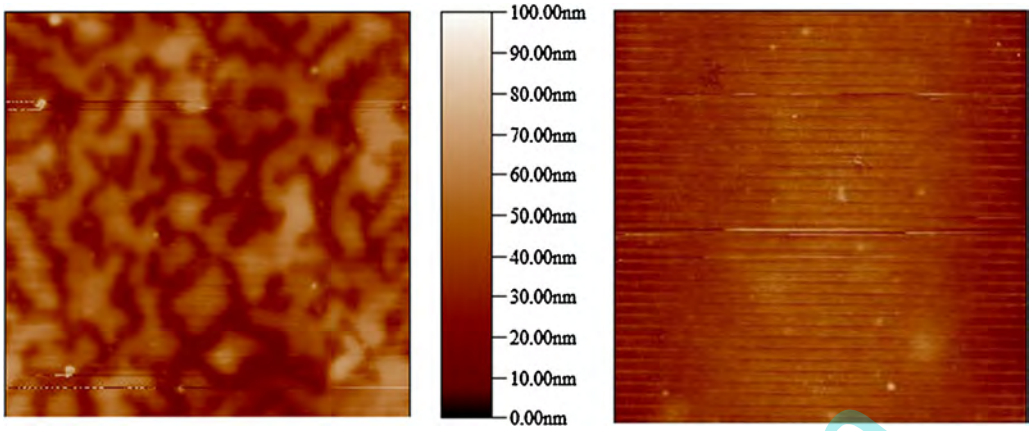

Fig. 3. AFM images of the surface morphology of gelatin-Ag NPs-0.7 films. The height image and phase image with a 100 nm × 100 nm scale, respectively.

activity [36]. Because of the presence of active carboxyl, amino and hydroxyl functional groups, CCHI is an amphiprotic ionic polymer in aqueous solution and can react with other agents that contain amino or carboxyl groups, such as gelatin [41]. In this work, we chose CCHI as a surface-modification agent to form a CCHI film by electrostatic attraction on the gelatin-Ag NP films. Ag NP-containing hybrid films were obtained by placing each gelatin-Ag NP film in an aqueous solution of CCHI (1.5%, *w*/*w*) for 10 min. The CCHI molecules first interacted with the gelatin-Ag films by electrostatic attraction, and then formed covalent bonds between amino or carboxyl groups of CCHI and carboxyl or amino groups of gelatin [42,43]. As a control experiment, we also fabricated gelatin film, gelatin-CCHI films without Ag NPs and gelatin-Ag NPs film. They were produced in the same manner as the Ag NP-containing hybrid films.

The antibacterial properties of the gelatin-CCHI and Ag NP-containing hybrid films were tested by co-culturing with *E. Coli* bacteria. Fig. 4 shows colony images of *E. Coli* after control and co-culturing experiments. Colony counting showed that in the presence of gelatin film, there is almost no killing efficiency. When gelatin-CCHI film was co-cultured with *E. Coli*, the killing efficiency was about 37% after comparison with the control experiment. This result was mainly attributed to the antimicrobial effect of CCHI, which contains positively charged amino groups that can bind to the negatively charged bacterial cell membrane *via* electrostatic interaction, leading to the release of proteins and other constituents of the bacterial cell and inhibiting nutrient transport [44,45]. The antibacterial activity of gelatin-Ag NPs film without CCHI was measured, and its efficiency was about 90%. After CCHI was covered onto the gelatin-Ag NPs film, the antibacterial efficiency reached nearly 100% when the Ag NP hybrid film was added to an *E. Coli* suspension. This hybrid film combined Ag NP with CCHI showed the best antibacterial efficiency.

3.3. MEF of gelatin-Ag NP-CCHI/OFBT-AA films

To study the MEF of the Ag NP hybrid film, conjugated oligomer OFBT-AA was chosen as a model dye because its emission

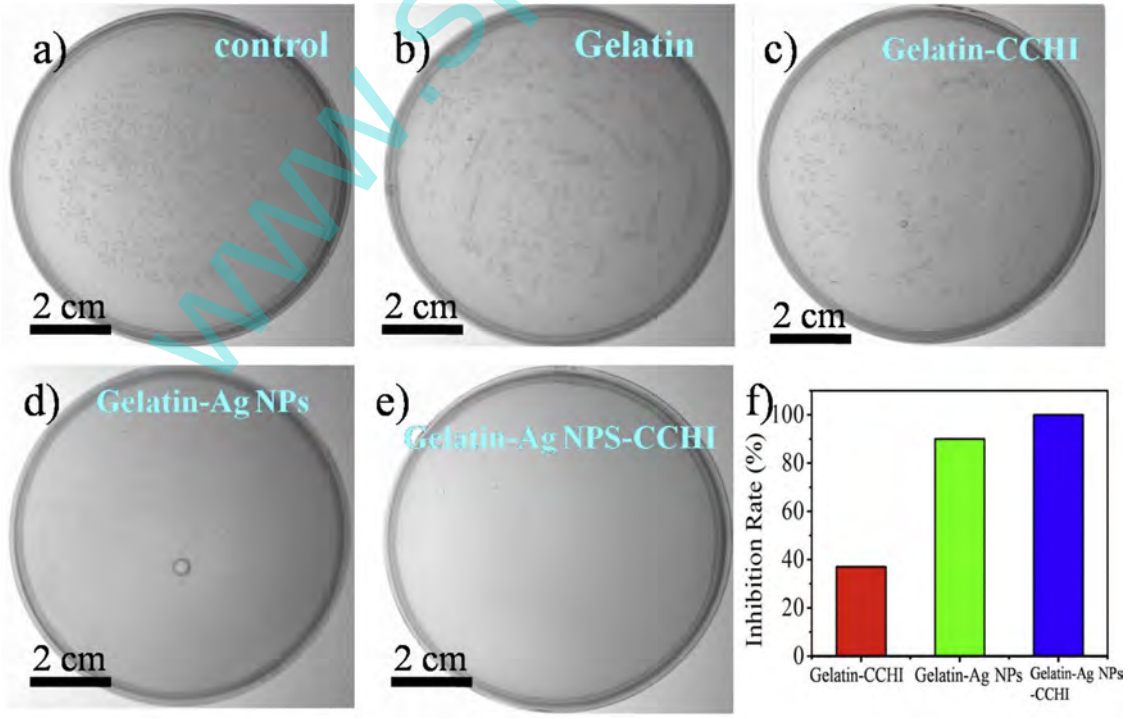

Fig. 4. Photographs of *E. Coli* agar plates treated (a) without anything, (b) with gelatin film, (c) with gelatin-CCHI film, (d) with gelatin-Ag NPs film and (e) with gelatin-Ag NPs-CCHI hybrid film. (f) Biocidal activity of gelatin-CCHI, gelatin-Ag NPs film and gelatin-Ag NPs-CCHI hybrid films toward *E. Coli*.

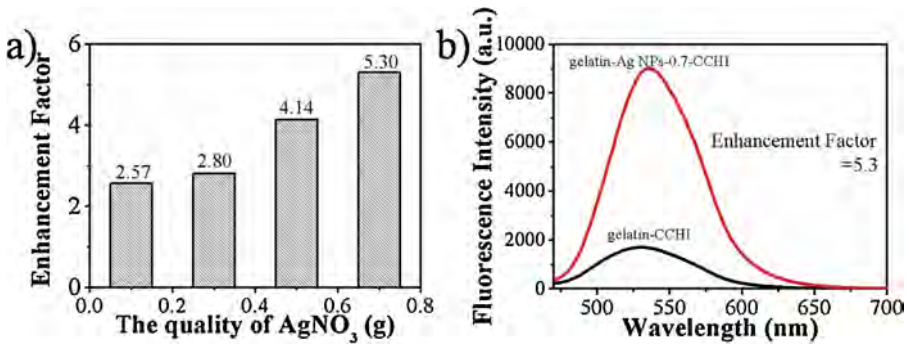

Fig. 5. (a) Enhancement factor of gelatin-CCHI films with different amounts of Ag NPs, and (b) fluorescence spectra of OFBT-AA in the presence of Ag NPs-0.7 hybrid and gelatin-CCHI films.

spectrum is close to the absorption spectrum of the gelatin-coated Ag NPs, and its small π-conjugated structure is suitable for MEF in films [46,47]. CCHI molecules were absorbed on the prepared gelatin-Ag NPs film as the interlayer between Ag NPs and fluorescent dyes. If there is no interlayer between fluorophore and AgNPs, the fluorescence of fluorophore will be quenched directly. Before detecting fluorescence spectra, the gelatin-Ag NP-CCHI films were heated for 1 h at 45 °C to remove water. An aqueous solution of OFBT-AA was added and absorbed onto the surface of each dried hybrid film, and then each film was dried under a flow of air at room temperature for 2 h. For comparison, a dried gelatin-CCHI film with the same amount of OFBT-AA dye was also prepared. The dye-marked films were excited at 427 nm, which is the maximum absorption wavelength of OFBT-AA. Fluorescence spectra of gelatin-CCHI films containing different amounts of Ag NPs were also measured. The fluorescence enhancement factor is defined as I/I_0, where I is the emission intensity of OFBT-AA (2 μL, 1 mM) after loading in each gelatin-Ag NP-CCHI film, and I_0 is the emission intensity of OFBT-AA (2 μL, 1 mM) in gelatin-CCHI film. According to this calculation method, the fluorescence enhancement factors of gelatin-CCHI with of 0.1, 0.3, 0.5 and 0.7 g of $AgNO_3$ used to prepare Ag NPs were 2.57, 2.80, 4.14 and 5.3, respectively (Fig. 5a). Fig. 5b depicts the fluorescence spectra of OFBT-AA in the presence of Ag NPs-0.7 hybrid and gelatin-CCHI films. The fluorescence intensity of OFBT-AA was obviously increased a maximum 5.3-fold in the presence of Ag NPs. According to our previous work [39], the increased fluorescence intensity of OFBT-AA may be attributed to two effects. Ag NPs present as a surface plasmon resonance source may increase the excitation efficiency or decrease the nonradiative decay of the dye. With increased content of Ag NPs, larger fluorescence enhancement can be obtained. This is because the more Ag NPs present to act as a surface plasmon resonance source, the higher the MEF effect of the Ag NP hybrid film [48].

The distance between metal and dye is a very important factor in MEF. If the dye is too close to the metal, fluorescence is quenched, whereas there is no interaction if the distance is too large. Therefore, MEF is only detected when the metal–dye distance is within a certain range. In this system, the Ag NPs were synthesized by an *in situ* method and dispersed randomly in gelatin films. Thus, the observation of fluorescence enhancement indicated that the average distance between the Ag NPs and OFBT-AA dye molecules was suitable for MEF.

4. Conclusion

In summary, a facile, *in situ* and green approach to fabricate antibacterial and MEF-functional Ag NP hybrid films was developed. Natural biomacromolecule gelatin was used as a reduction agent and stabilizer for Ag NPs, while CCHI was used as a surface-modification layer. The resulting Ag NP hybrid films exhibited excellent antibacterial activity towards *E. Coli* with an inhibition ratio close to 100%. The hybrid films also display a MEF effect. The fluorescence enhancement factor increased with the Ag NP content of the film, with a maximum fluorescence enhancement factor of 5.3. These novel hybrid films could be applied in biomedical engineering and as bio-antibacterial materials.

Acknowledgements

This work is supported by the Fundamental Research Funds for the Central Universities. We are grateful to Dr. Libing Liu and Ms. Huanxiang Yuan for their kind support for the antibacterial experiments.

References

[1] K.M. Blair, L. Turner, J.T. Winkelman, H.C. Berg, D.B. Kearns, A molecular clutch disables flagella in the *Bacillus subtilis* biofilm, Science 320 (2008) 1636–1638.
[2] D.H. Bartlett, F. Azam, Chitin, cholera, and competence, Science 310 (2005) 1775–1777.
[3] A.M. Ferreira, I. Carmagnola, V. Chiono, P. Gentile, L. Fracchia, C. Ceresa, G. Georgiev, G. Ciardelli, Surface modification of poly(dimethylsiloxane) by two-step plasma treatment for further grafting with chitosan–rose bengal photosensitizer, Surf. Coat. Technol. 223 (2013) 92–97.
[4] M. Kammoun, M. Haddar, T.K. Kallel, M. Dammak, A. Sayari, Biological properties and biodegradation studies of chitosan biofilms plasticized with PEG and glycerol, Int. J. Biol. Macromol. 62 (2013) 433–438.
[5] M.A. TerAvest, Z. He, M.A. Rosenbaum, E.C. Martens, M.A. Cotta, J.I. Gordon, L.T. Angenent, Regulated expression of polysaccharide utilization and capsular biosynthesis loci in biofilm and planktonic *Bacteroides thetaiotaomicron* during growth in chemostats, Biotechnol. Bioeng. 111 (2014) 165–173.
[6] P. Veiga-Santos, M.P. Cereda, A.R.P. Scamparini, Cassava starch-gelatin bio based films structural stability and color during storage, Boletim do Centro de Pesquisa 26 (2008) 123–134.
[7] P. Saint-Cricq, J.Z. Wang, A. Sugawara-Narutaki, A. Shimojima, T. Okubo, A new synthesis of well-dispersed, core–shell Ag@SiO_2 mesoporous nanoparticles using aminoacids and sugars, J. Mater. Chem. B 1 (2013) 2451–2454.
[8] J. Xu, J.S. Yin, E. Ma, Nanocrystalline Ag formed by low-temperature high-energy mechanical attrition, Nanostract. Mater. 8 (1997) 91–100.
[9] J. Fitz-Gerald, S. Pennycook, H. Gao, R.K. Singh, Synthesis and properties of nanofunctionalized particulate materials, Nanostract. Mater. 12 (1999) 1167–1171.
[10] H.B. Chang, H.N. Sang, M.P. Seung, Formation of silver nanoparticles by laser ablation of a silver target in NaCl solution, Appl. Surf. Sci. 197-198 (2002) 628–634.
[11] J. Zhang, P. Chen, C. Sun, X. Hu, Sonochemical synthesis of colloidal silver catalysts for reduction of complexing silver in DTR system, Appl. Catal. A 266 (2004) 49–54.
[12] V.R. Chaudhari, S.K. Haram, S.K. Kulshreshtha, Micelle assisted morphological evolution of silver nanoparticles, Colloid Surf. A: Physicochem. Eng. Aspects 301 (2007) 475–480.
[13] A. Pal, S. Shah, S. Devi, Synthesis of Au, Ag and Au–Ag alloy nanoparticles in aqueous polymer solution, Colloid Surf. A: Physicochem. Eng. Aspects 302 (2007) 51–57.
[14] Z. Chen, L. Gao, A. Facile, Novel way for the synthesis of nearly monodisperse silver nanoparticles, Mater. Res. Bull. 42 (2007) 1657–1661.
[15] A. Kumar, H. Joshi, R. Pasricha, A.B. Mandale, M. Sastry, Phase transfer of silver nanoparticles from aqueous to organic solutions using fatty amine molecules, J. Colloid Interface Sci. 264 (2003) 396–401.

[16] D. Li, S. Chen, S. Zhao, X. Hou, H. Ma, X. Yang, Simple method for preparation of cubic Ag nanoparticles and their self-assembled films, Thin Solid Films 460 (2004) 78–82.
[17] X. Zhang, Z. Li, X. Yuan, Z. Cui, H. Bao, X. Li, Y. Liu, X. Yang, Cytotoxicity and antibacterial property of titanium alloy coated with silver nanoparticle-containing polyelectrolyte multilayer, Mater. Sci. Eng. C 33 (2013) 2816–2820.
[18] B. Xia, Q. Cui, F. He, L. Li, Preparation of hybrid hydrogel containing Ag nanoparticles by a green in situ reduction method, Langmuir 28 (2012) 11188–11194.
[19] B. Xia, F. He, L. Li, Preparation of bimetallic nanoparticles using a facile green synthesis method and their application, Langmuir 29 (2013) 4901–4907.
[20] Y. Liu, X. Liu, X. Wang, Biomimetic synthesis of gelatin polypeptide assisted noble-metal nanoparticles and their interaction study, Nanoscale Res. Lett. 6 (2011) 22.
[21] R.J.B. Pinto, S.C.M. Fernandes, C.S.R. Freire, P. Sadocco, J. Causio, C.P. Neto, T. Trindade, Antibacterial activity of optically transparent nanocomposite films based on chitosan or its derivatives and silver nanoparticles, Carbohydr. Res. 348 (2012) 77–83.
[22] H.V. Tran, L.D. Tran, C.T. Ba, H.D. Vu, T.N. Nguyen, D.G. Pham, P.X. Nguyen, Synthesis, Characterization, antibacterial and antiproliferative activities of monodisperse chitosan-based silver nanoparticles, Colloid Surf. A: Physicochem. Eng. Aspects 360 (2010) 32–40.
[23] P. Kanmani, J.-W. Rhim, Physicochemical properties of gelatin/silver nanoparticle antimicrobial composite films, Food Chem. 148 (2014) 162–169.
[24] X. Wang, T.-T. Lim, Highly efficient and stable Ag/AgBr/TiO_2 composites for destruction of *Escherichia coli* under visible light irradiation, Water Res. 47 (2013) 4148–4158.
[25] V. Sambhy, M.M. MacBride, B.R. Peterson, A. Sen, Silver bromide nanoparticle/polymer composites: dual action tunable antimicrobial materials, J. Am. Chem. Soc. 128 (2006) 9798–9808.
[26] Y. Fu, J. Zhang, J.R. Lakowicz, Largely enhanced single-molecule fluorescence in plasmonic nanogaps formed by hybrid silver nanostructures, Langmuir 29 (2013) 2731–2738.
[27] M.H. Chowdhury, K. Ray, K. Aslan, J.R. Lakowicz, C.D. Geddes, Metal-enhanced fluorescence of phycobiliproteins from heterogeneous plasmonic nanostructures, J. Phys. Chem. C 111 (2007) 18856–18863.
[28] S.D. Choudhury, R. Badugu, K. Ray, J.R. Lakowicz, Silver–gold nanocomposite substrates for metal-enhanced fluorescence: ensemble and single-molecule spectroscopic studies, J. Phys. Chem. C 116 (2012) 5042–5048.
[29] F. Tang, F. He, H. Cheng, L. Li, Self-assembly of conjugated polymer-Ag@SiO_2 Hybrid fluorescent nanoparticles for application to cellular imaging, Langmuir 26 (2010) 11774–11778.
[30] F. Tang, N. Ma, X. Wang, F. He, L. Li, Hybrid conjugated polymer-Ag@PNIPAM fluorescent nanoparticles with metal-enhanced fluorescence, J. Mater. Chem. 21 (2011) 16943–16948.
[31] J. Zhang, N. Ma, F. Tang, Q. Cui, F. He, L. Li, pH- and glucose-responsive core–shell hybrid nanoparticles with controllable metal-enhanced fluorescence effects, ACS Appl. Mater. Interfaces 4 (2012) 1747–1751.
[32] L. Li, F. He, X. Wang, N. Ma, L. Li, Reversible pH-responsive fluorescence of water-soluble polyfluorenes and their application in metal ion detection, ACS Appl. Mater. Interfaces 4 (2014) 4927–4933.
[33] X. Wang, F. He, L. Li, H. Wang, R. Yan, L. Li, Conjugated oligomer-based fluorescent nanoparticles as functional nanocarriers for nucleic acids delivery, ACS Appl. Mater. Interfaces 5 (2013) 5700–5708.
[34] B. Xia, X. Wang, F. He, Q. Cui, L. Li, Self-Assembly of conjugated polymer on hybrid nanospheres for cellular imaging applications, ACS Appl. Mater. Interfaces 4 (2012) 6332–6337.
[35] H. Yuan, H. Chong, B. Wang, C. Zhu, L. Liu, Q. Yang, F. Lv, S. Wang, Chemical molecule-induced light-activated system for anticancer and antifungal activities, J. Am. Chem. Soc. 134 (2012) 13184–13187.
[36] S.-K. Kim, E. Mendis, Bioactive compounds from marine processing byproducts—a review, Food Res. Int. 39 (2006) 383–393.
[37] E. Mendis, N. Rajapakse, S.-K. Kim, Evaluation of the effect of germination on phenolic compounds and antioxidant activities in sorghum varieties, J. Agric. Food Chem. 53 (2004) 2581–2587.
[38] A. Pourjavadi, R. Soleyman, Silver nanoparticles with gelatin nanoshells: photochemical facile green synthesis and their antimicrobial activity, J. Nanopart. Res. 13 (2011) 4647–4658.
[39] N. Ma, F. Tang, X. Wang, F. He, L. Li, Tunable metal-enhanced fluorescence by stimuli-responsive polyelectrolyte interlayer films, Macromol. Rapid Commun. 32 (2011) 587–592.
[40] L. Tong, N. Ma, F. Tang, D. Qiu, Q. Cui, L. Li, pH and thermoresponsive Ag/polyelectrolyte hybrid thin films for tunable metal-enhanced fluorescence, J. Mater. Chem. 22 (2012) 8988–8993.
[41] D.S. dos Santos, P.J.G. Goulet, N.P.W. Pieczonka, O.N. Oliveira, R.F. Aroca, Gold nanoparticle embedded, self-sustained chitosan films as substrates for surface-enhanced Raman scattering, Langmuir 20 (2004) 10273–10277.
[42] F.-L. Mi, Synthesis and characterization of a novel chitosan–gelatin bioconjugate with fluorescence emission, Biomacromolecules 6 (2005) 975–987.
[43] S. Rinaldi, E. Fortunati, M. Taddei, J.M. Kenny, I. Armentano, L. Latterini, Integrated PLGA–Ag nanocomposite systems to control the degradation rate and antibacterial properties, J. Appl. Polym. Sci. 130 (2013) 1185–1193.
[44] D. Celis, M.I. Azocar, J. Enrione, M. Paez, S. Matiacevich, Characterization of salmon gelatin based film on antimicrobial properties of chitosan against *E. coli*, Procedia Food Sci. 1 (2011) 399–403.
[45] T. Chen, R. Wang, L. Xu, K.G. Neoh, E.-T. Kang, Carboxymethyl chitosan-functionalized magnetic nanoparticles for disruption of biofilms of *Staphylococcus aureus* and *Escherichia coli*, Ind. Eng. Chem. Res. 51 (2012) 13164–13172.
[46] C. Zhu, L. Liu, Q. Yang, F. Lv, S. Wang, Water-soluble conjugated polymers for imaging, diagnosis, and therapy, Chem. Rev. 112 (2012) 4687–4735.
[47] Q. Cui, F. He, L. Li, H. Möhwald, Controllable metal-enhanced fluorescence in organized films and colloidal system, Adv. Colloid Interface Sci. 207 (2014) 164–177.
[48] X. Wang, F. He, X. Zhu, F. Tang, L. Li, Hybrid silver nanoparticle/conjugated polyelectrolyte nanocomposites exhibiting controllable metal-enhanced fluorescence, Sci. Rep. 4 (2014) 4406.